

Specific molecular and cellular events induced by irradiated X-ray photoactivatable drugs raise the problem of co-toxicities: particular consequences for anti-cancer synchrotron therapy

Jérôme Gastaldo,^a Zuzana Bencokova,^a Catherine Massart,^a Aurélie Joubert,^b Jacques Balosso,^c Anne-Marie Charvet^a and Nicolas Foray^{a*}

^aINSERM, U836, Institut des Neurosciences, 38043 Grenoble, France, ^bSociété Magelis, 84160 Cadenet, France, and ^cDépartement de Radiothérapie, Centre Hospitalo Universitaire, 38042 Grenoble, France. E-mail: nicolas.foray@inserm.fr

Synchrotrons are capable of producing intense low-energy X-rays that enable the photoactivation of high-*Z* elements. Photoactivation therapy (PAT) consists of loading tumors with photoactivatable drugs and thereafter irradiating them at an energy, generally close to the *K*-edge of the element, that enhances the photoelectric effect. To date, three major photoactivatable elements are used in PAT: platinum (cisplatin and carboplatin), iodine (iodinated contrast agents and iododeoxyuridine) and gadolinium (motexafin gadolinium). However, the molecular and cellular events specific to PAT and the radiobiological properties of these photoactivatable drugs are still unknown. Here, it is examined how standard and synchrotron X-rays combined with photoactivatable drugs impact on the cellular response of human endothelial cells. These findings suggest that the radiolysis products of the photoactivatable drugs may participate in the synergetic effects of PAT by increasing the severity of radiation-induced DNA double-strand breaks. Interestingly, subpopulation of highly damaged cells was found to be a cellular pattern specific to PAT. The data show that the efficiency of emerging anti-cancer modalities involving synchrotron photoactivation strongly depends on the choice of photoactivatable drugs, and important series of experiments are required to secure their clinical transfer before applying to humans.

© 2011 International Union of Crystallography
Printed in Singapore – all rights reserved

Keywords: photoactivation; DNA double-strand breaks; toxicity.

1. Introduction

To date, there is documented evidence that chemotherapy combined with radiation treatment is more efficient in treating cancer than both modalities applied separately. A representative example is given by cisplatin that provides a supra-additive effect when applied concomitantly with radiotherapy (Corde *et al.*, 2003; Biston *et al.*, 2004, 2009). For several decades now, treatments based on the X-ray photoactivation of high-*Z* elements have been proposed (Fairchild & Bond, 1984). This approach, called photon activation therapy (PAT), was postulated as increasing the supra-additivity of the combination of radiation with a chemotherapy drug by inducing a photoelectric effect using low-energy X-rays to produce additional damage into tumors. Such low-energy X-rays can be produced either in a polychromatic spectrum by CT scanners or as monochromatic beams by synchrotrons (Bencokova *et al.*, 2008; Foray, 2010).

The photoactivatable drugs that have already been tested for PAT are halogenated base analogs like iododeoxyuridine (IUdR) (Miller *et al.*, 1987), iodinated contrast agents (Joubert *et al.*, 2005), platinum salts radiotherapy (Biston *et al.*, 2009, and references herein) and gadolinium porphyrins (De Stasio *et al.*, 2006). All these drugs are photoactivatable by X-rays at an energy corresponding either to the inner-shell *K*-edge of the element or to the maximal energy absorption of this element in water. Further investigations are, however, needed to better understand the physical and biochemical mechanisms involved in the PAT modalities in order to secure their clinical transfer. The concomitant use of radiation and photoactivatable high-*Z* elements raises three major questions, at least. (i) Are there any molecular and cellular events that are specific to the photoactivation of high-*Z* elements? (ii) Can the energy produced by the photoactivatable drug lead to its photodecomposition? (iii) If yes, do the resulting radiolytic products contribute to supra-additive effects?

Recent advances in radiobiology have provided new tools to better evaluate the molecular and cellular response of such combined treatments and any related aspects from the radiation- and chemical-induced stress. Specifically, immunofluorescence techniques can be used to provide the choreography of individual DNA damage. Among the molecular markers of toxicity, the phosphorylation of the variant X of the H2A histone (γ -H2AX) was shown to reflect the recognition of DNA double-strand breaks (DSBs) that are the key events of cellular death (Rothkamm & Lobrich, 2003; Joubert *et al.*, 2008). Here, we analyzed the yield of DSBs based upon γ -H2AX immunofluorescence and some specific morphological features that occur in irradiated cells after treatment with some of the most extensively used photoactivatable drugs. Four photoactivatable elements complexed with different photoactivatable drugs were considered: iodine [with iododeoxyuridine (IUdR) and iomeprol, an iodinated contrast agent], platinum (with cisplatin) and gadolinium (with motexafin, a gadolinium-containing contrast agent). The present paper represents the first systematic study dealing with the potential toxicity of the most widely used molecules as potential clinical candidates for PAT.

2. Materials and methods

2.1. Cell line and drugs

In order to investigate the biomolecular events specific to PAT and to secure the clinical transfer of PAT modalities, and since some contrast agents are injected intravenously, the endothelial HMEC cell line from human normal tissues was chosen. HMEC cells were routinely cultured as monolayers with RPMI medium (Gibco-Invitrogen-France, Cergy-Pontoise, France), supplemented with 20% fetal calf serum, penicillin and streptomycin (Joubert *et al.*, 2005). All the experiments were performed with cells in the logarithmic phase of growth. Motexafin gadolinium (Pharmacyclics, Sunnyvale, CA, USA) and cisplatin as *cis*-diamminedichloroplatinum (II) (Cysplatyl) (Rhône-Poulenc, Rorer, Montrouge, France) were kindly provided by the Grenoble Hospital (Grenoble, France). Iomeprol (Iomeron 350) was purchased from Bracco (Milan, Italy) and IUdR from Sigma-Aldrich (Sigma-France, L'Isle d'Abeau, France). All experiments were performed at a drug concentration of 30 μ M.

2.2. Standard X-ray irradiations

An X-ray clinical irradiator devoted to research was used to perform all the irradiations. The X-ray beam was produced from a tungsten anode, applying a voltage setting of 200 kV, an intensity of 20 mA and using a filtration of 0.1 mm copper filter. The dose rate was 1.234 Gy min⁻¹ (Joubert *et al.*, 2005).

2.3. Synchrotron X-ray irradiations

Synchrotron X-ray irradiation was performed at the ID17 beamline of the European Synchrotron Radiation Facility (Grenoble, France). The irradiation protocol has been detailed elsewhere (Biston *et al.*, 2009). Briefly, cells were in

suspension in rotating plastic tubes and irradiated at 277 K. The beam size (1 mm high) and its homogeneous part (8 cm wide) allowed two tubes to be irradiated simultaneously by vertical scanning. A cylindrical ionizing chamber coupled with a UNIDOS electrometer and high-purity germanium detector (Eurisy Mesure, Lingolsheim, France) were used for radiation dose calibration. The beam energy was tuned to the indicated X-ray energy with an energy bandwidth of 80 eV.

2.4. Flow cytometry

About 5×10^5 cells were seeded onto a 100 mm dish. After treatment, cells were trypsinized and fixed with ice-cold 70% ethanol at a density of 5×10^5 cells ml⁻¹ and stored at 253 K. Before analysis, cells were resuspended in 0.1 ml of PBS and stained with propidium iodide (5 μ g ml⁻¹) in the presence of 50 μ g ml⁻¹ RNase. At least 10^4 cells were analysed using a FACS Calibur flow cytometer (Becton Dickinson-France, Pont de Claix, France) and *WinMDI 2.8* software (Scripps Research Institute, La Jolla, CA, USA) (Foray *et al.*, 1999).

2.5. Immunofluorescence

The immunofluorescence protocol employed was described elsewhere (Foray *et al.*, 2003; Joubert *et al.*, 2008). Cells were fixed in 3% paraformaldehyde, 2% sucrose PBS for 15 min at room temperature and permeabilized in 20 mM HEPES, pH 7.4, 50 mM NaCl, 3 mM MgCl₂, 300 mM sucrose 0.5% Triton X-100 (Sigma-Aldrich, L'Isle d'Abeau-Chesne, France) for 3 min at 277 K. Thereafter, coverslips were washed in PBS prior to immunostaining. Primary antibody incubations were performed for 40 min at 310 K in PBS supplemented with 2% bovine serum fraction V albumin (BSA) (Sigma-Aldrich) and followed by PBS washing. Anti- γ -H2AX^{ser139} antibody was purchased from Upstate Biotechnology-Euromedex (Mundolsheim, France) and diluted 1:800. Incubations with anti-mouse FITC secondary antibodies (Sigma-Aldrich) (dilution 1:100) were performed at 310 K in 2% BSA for 20 min. Slides were mounted in 4',6'-diamidino-2-phenylindole (DAPI)-stained Vectashield (Abcys) and examined with an Olympus fluorescence microscope. One hundred nuclei per treatment were analyzed by eye and confirmed by *ImageJ* free software. DAPI staining permitted an indirect evaluation of the yield of G₁ cells (nuclei with homogeneous DAPI staining), S cells (nuclei showing numerous pH2AX foci), G₂ cells (nuclei with heterogeneous DAPI staining) and metaphase (visible chromosomes). During the experiments with γ -H2AX immunofluorescence, we observed a subpopulation of cells exhibiting so many γ -H2AX foci (more than 50) that their number was almost impossible to determine with precision. Inside these highly damaged cells (HDCs) the pattern of γ -H2AX foci was unusual, with a filamentous aspect and high fluorescence intensity. The detection of HDC was easily detectable since the size of the nucleus was 1.5–3 times larger than average.

3. Results

3.1. Reparability of 250 kV X-ray-induced DSBs after pre-incubation of cells with photoactivatable drugs

As a first step, we investigated the repair rate of DSBs induced by 250 kV X-ray irradiation in endothelial HMEC cells after a 24 h pre-incubation of non-irradiated photoactivatable drugs and renewal of the culture medium immediately before the irradiation. The repair rate of DSBs was assessed with the γ -H2AX immunofluorescence technique. A 24 h pre-incubation of the contrast agents, iomeprol and motexafin gadolinium, that do not naturally enter into cells, did not affect the DSB repair rate. Conversely, the pre-incubation of chemotherapeutic drugs like cisplatin, whose penetrability into cells and DNA binding capacity is well documented, disturbed the DSB repair rate by increasing the severity of DSBs (Biston *et al.*, 2009) (Fig. 1*a*). IUdR also affected the DSB repair rate but at a lesser extent than cisplatin. Interestingly, when irradiation was performed in the presence of the photoactivatable drugs after a 24 h pre-incubation (*i.e.* without renewal of culture medium), the severity of DSBs was increased in all the cases but the effect was less impressive with iomeprol and motexafin gadolinium (Fig. 1*b*).

Altogether, these data suggest that the severity of DSBs may change dramatically depending upon the photoactivatable drug used and its interaction with radiation. While the data with iomeprol, cisplatin and IUdR were reported in previous papers (Joubert *et al.*, 2005; Biston *et al.*, 2004; Kinsella *et al.*, 1987), the motexafin gadolinium data are new. Our results suggest that motexafin gadolinium impacts on the

DSB repair rate and, consequently, may be advantageous for cancer treatment but raises questions about its toxicity for normal tissues when used in conjunction with procedures involving radiation. Since motexafin gadolinium, similarly to iomeprol, does not penetrate cells spontaneously, our data suggest two possible scenarios: (i) irradiation causes radiolysis of the drug and the resulting radiolytic compounds are then able to enter into the cells and inhibit the DSB repair rate, and/or (ii) irradiation increases the penetrability of the drug into the cells (at least transiently) as a result of membrane permeabilization and thereby inhibits the DSB repair rate.

In order to investigate the relevance of these two scenarios, photoactivatable drugs were irradiated in solution and applied directly to non-irradiated cells. With the notable exception of motexafin gadolinium, with which about two additional γ -H2AX foci per cell were observed, no significant increase in the number of γ -H2AX foci and no micronuclei was found with all other compounds, suggesting that they do not penetrate into the cells or that radiation may have affected the integrity of the compounds themselves. Neither do these compounds produce, *per se*, a significant yield of DSBs if the cells are not irradiated (data not shown). Thereafter, to estimate the impact of radiation-induced membrane permeabilization, photoactivatable drugs in solution and cells in their culture medium were irradiated *separately* and then combined at intervals corresponding to 10 min, 1 h or 4 h after irradiation. Such treatment impacted on the DSB repair rate with great diversity among the different compounds (Fig. 2). With cisplatin, the DSB repair rate was decreased when the drug and cells were combined at 10 min or 1 h after irradiation.

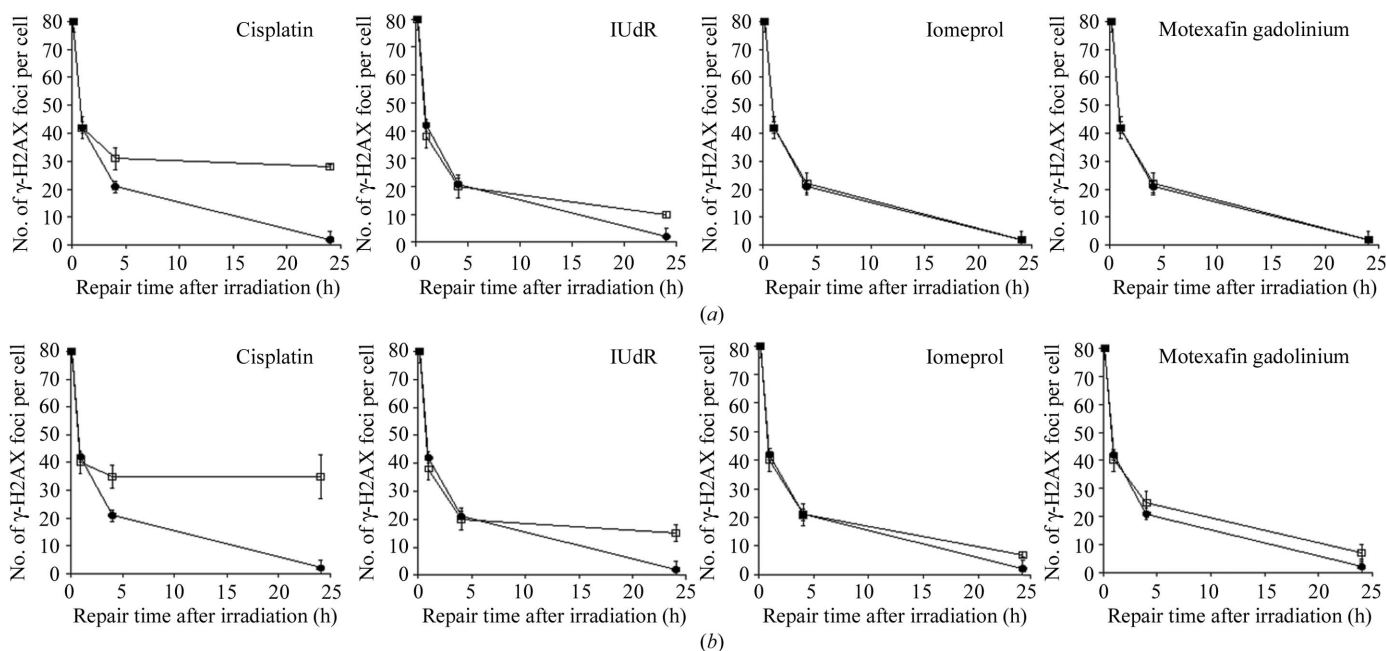


Figure 1 Data are expressed as the number of γ -H2AX foci per cell plotted against repair time post-irradiation. Each plot represents the mean \pm standard errors of at least two independent replicates. (a) HMEC cells were pre-incubated for 24 h with 30 μ M of platin, iodine (IUdR and iomeprol) or gadolinium. Immediately before the exposure to a total dose of 2 Gy 250 kV X-rays, the cell medium was renewed without drug. (b) The experimental protocols for curves in (a) and (b) were the same with the exception that the cell medium was not renewed in the (b) experiments and the photoactivatable drug was present during the irradiation and for an additional 24 h. Closed circles and open squares correspond to conditions without and with drugs, respectively.

No specific effect was observed when the mixture was performed 4 h after irradiation. Iomeprol significantly decreased the DSB repair rate only at the 1 h time point. With both IUdR and motexafin gadolinium, the DSB repair rate was significantly decreased only at the 10 min interval (Fig. 2). No matter which of the photoactivatable drugs was used, it appears that the irradiation of the photoactivatable drugs and cells *separately* enhances the severity of the radiation-induced DSBs. Altogether, these data suggest that irradiation of the photoactivatable drug may produce toxic products and may help these products to penetrate into cells. However, the intensity of the radiosensitizing effect strongly depends on the nature of the photoactivatable drug itself.

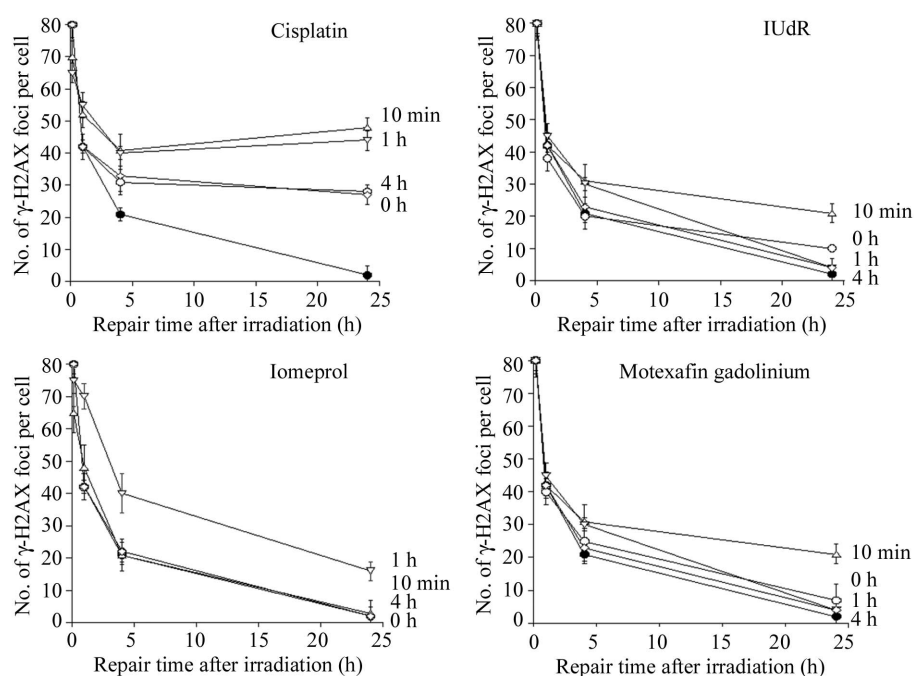


Figure 2

Data are expressed as the number of γ -H2AX foci per cell plotted against repair time post-irradiation. Each plot represents the mean \pm standard errors of two independent replicates at least. HMEC cells and solutions of photoactivatable drugs were exposed to 2 Gy 250 kV X-rays separately. The pre-irradiated drug solution was applied to culture medium at the indicated post-irradiation times and measured for DSBs at 4 and 24 h. Closed circles and open squares correspond to conditions without and with drugs, respectively. It is noteworthy that the data plots labelled '0 h' are the same as those shown in Fig. 1(b).

3.2. Specific observations of highly damaged cells (HDCs)

HDCs were mainly observed at 10 min and 1 h post-irradiation and appeared also to be dependent on the nature of the particular drug [Figs. 3(a) and 3(b)]. In order to examine the relationship between HDCs and DSBs, we plotted the percentage of HDCs at 0, 10 min, 1 h and 4 h post-irradiation against the corresponding number of γ -H2AX foci obtained for the different drug treatments shown in Fig. 1(b). The number of unrepaired DSBs was found to be globally proportional ($r = 0.72$ when all data were gathered) to the occurrence of HDCs (Fig. 3c). Altogether, these data suggest that the yield of HDCs increases with the severity of DSBs and might be the result of an uncontrolled nuclease activity in response to unrepairable DSBs, as has been suggested earlier (Thomas *et al.*, 2008), that may lead to a severe chromatin decondensation. Hence, the yield of HDCs may serve also as a sensor of toxicity for radiochemotherapy involving photoactivatable drugs.

The DAPI counterstaining used in our immunofluorescence experiments provided information on both the shape of nuclei and the phase of the cell cycle in which the cells are found. Immunofluorescence indicated that HDC nuclei were about 1.5 times larger than average and observed in G0/G1 since DAPI staining was homogeneous (Thomas *et al.*, 2008). HDCs were not apoptotic bodies. To consolidate this conclusion and examine whether cell cycle distribution is affected when HDCs occurred, flow cytometry was applied 24 h after separated irradiation of cells and photoactivatable drugs followed by a mix 1 h after irradiation. Cell cycle arrests and sub-population in sub-G1 reflecting apoptosis were not significant (Fig. 4).

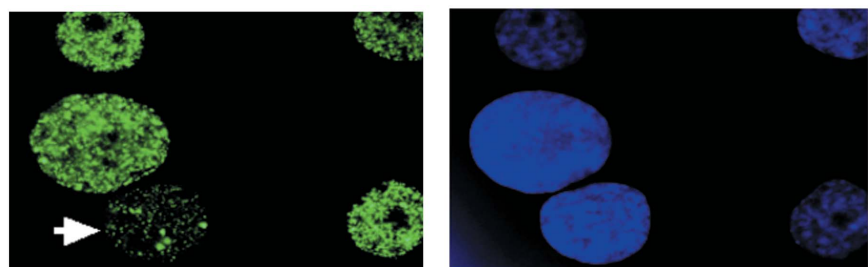
3.3. Photoactivation with synchrotron X-rays

To examine whether HDCs are also observed during photoactivation induced by synchrotron X-rays, we subjected cells to 30 μ M cisplatin for 24 h and irradiated them with synchrotron X-rays at different energies ranging between 20 and 90 keV. It is to be noted that 78.4 keV corresponds to the *K*-edge of platinum atoms. The appearance of HDCs assessed 1 h post-irradiation was similar to that observed when cells and drugs were irradiated separately as described above. The closer the X-ray energy was to the *K*-edge of Pt, the greater the number of HDCs. The number of HDCs reached its maximum at the *K*-edge. The number of HDCs at the *K*-edge was significantly higher than those assessed with 250 kV X-rays and than any other synchrotron X-ray energy tested, to the notable exception of 78.8 keV (no statistical difference) (Fig. 5).

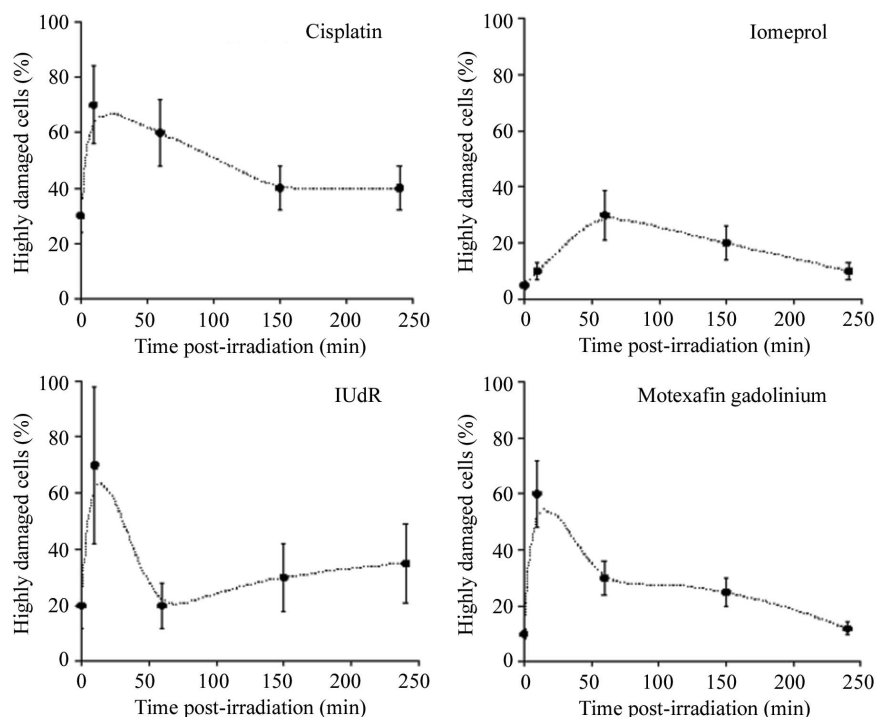
4. Discussion

4.1. Co-toxicity depending on the nature of the photoactivatable drugs

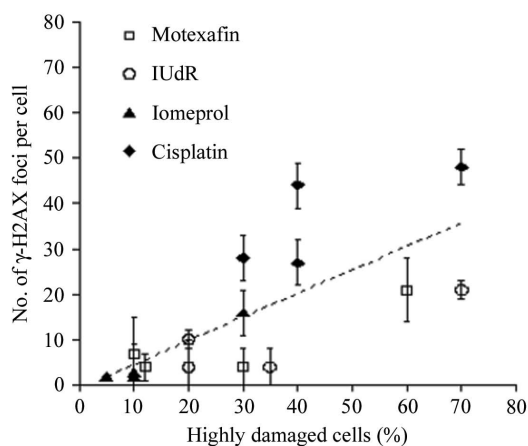
To date, four studies dealing with photoactivation of platinated and iodinated drugs provide mechanistic models of PAT (Joubert *et al.*, 2005; Corde *et al.*, 2003; Biston *et al.*, 2004, 2009). With regard to platinated drugs, the induced DSBs are more slowly repairable owing to the formation of cisplatin-



(a)



(b)



(c)

Figure 3

(a) Representative examples of HDCs observed with γ -H2AX immunofluorescence, stained in green (FITC) and counterstained with DAPI (blue). The nucleus marked by the white arrow was not considered as HDCs. (b) Percentage of HDC as a function of post-irradiation time for each photoactivatable drug irradiated separately and added directly to the culture medium at the indicated times (corresponding γ -H2AX data are shown in Fig. 2). Each plot represents the mean \pm standard errors of two independent replicates at least. (c) The percentage of HDC assessed at 0, 10 min, 1 h and 4 h post-irradiation shown in (b) were plotted against the corresponding γ -H2AX data shown in Fig. 1(b). Dotted lines correspond to linear regression when all data were gathered ($r = 0.75$).

DNA adducts that prevent the translocation of the Ku repair protein onto DNA (Turcchi *et al.*, 2000). Since the Ku protein is an essential element of the DNA-PK complex, a major component of the non-homologous end-joining (NHEJ) DSB repair pathway, the excess of unrepaired DSBs in irradiated cells after pre-treatment for 24 h with cisplatin is an important observation.

Regarding the photoactivation of iodine, it has been shown that iomeprol does not enter spontaneously into cells and its presence in culture medium for 24 h does not create DSBs. Furthermore, the photoactivation of iodine atoms harbored by iomeprol causes its photodegradation yielding free iodine ions. These iodine ions naturally tend to bind to potassium and sodium contained in the medium. The resulting iodides are therefore able to penetrate into the cells, bind and precipitate DNA and inhibit the DNA-PK kinase activity, similarly to cisplatin (Joubert *et al.*, 2005). As a result, NHEJ is inhibited explaining also the yield of unrepaired DSBs. Hence, conversely to cisplatin, in the case of iodinated contrast agents, the molecules that lead to toxicity are not iodinated contrast agents themselves but their radiolytic compounds. This assumption was confirmed by two types of experiments: (i) the irradiation of iodinated contrast agents and cells separately that demonstrated a decrease in the DSB repair rate; (ii) the addition of the irradiated contrast agent solution or iodides as NaI or KI, in the culture medium, that caused a significant deceleration of the DSB repair rate even 3 h after irradiation (Joubert *et al.*, 2005). It is also noteworthy that IUdR, as halogenated pyrimidine, binds naturally DNA as well. Our data suggest that radiolysis of IUdR may also affect NHEJ *via* the inhibition of the DNA-PK activity and/or the release of free iodine ions to explain the data obtained with separated irradiations. However, further investigations are needed to confirm this hypothesis.

The toxicity of the motexafin gadolinium is well documented (De Stasio *et al.*, 2006; Feng *et al.*, 2010; Bradley *et al.*, 2008). Since motexafin is a porphyrin that triggers formation of radical

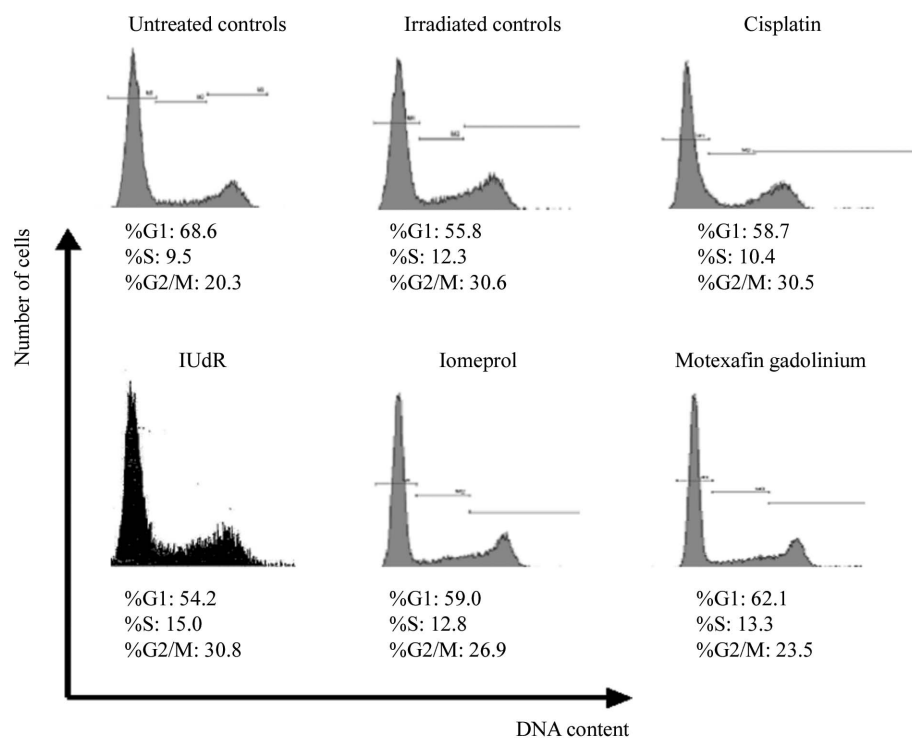


Figure 4 Representative cell cycle patterns of untreated cells, irradiated cells and irradiated cells (2 Gy) treated with an irradiated solution of photoactivatable drugs (2 Gy) 1 h after irradiation and fixed 24 h thereafter. The percentages of cells in the G1, S and G2/M phase are given for each situation. The percentage of sub-G1 cells was not significant, irrespective of the conditions.

oxygen species (ROS) when applied for at least 24 h (Feng *et al.*, 2010; Bradley *et al.*, 2008), it is not surprising that cells show some additional DSBs under our conditions. However, the photoactivation of motexafin gadolinium obeys a scenario different from that of cisplatin and iomeprol: unlike iomeprol, but more like cisplatin, the molecule shows some toxicity *per se*, and appears to penetrate into cells spontaneously to produce some DSBs. Unlike cisplatin, and more like iomeprol, the radiolytic compounds of motexafin gadolinium also appear

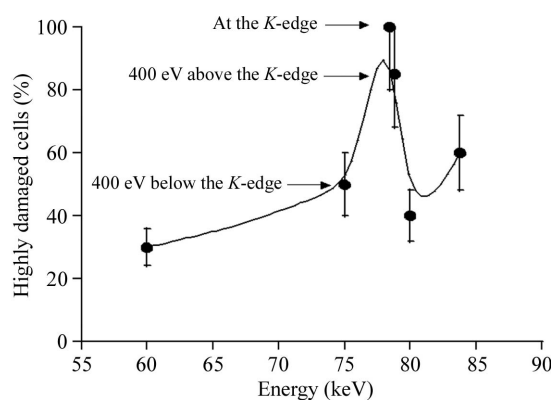


Figure 5 The percentage of HDCs found 1 h post-irradiation as a function of synchrotron X-rays energy observed in conditions of photoactivation of cisplatin (Biston *et al.*, 2004). A relative error of 15% was estimated for each condition.

to be toxic. These findings are consistent with the fact that motexafin gadolinium was shown to be a radiosensitizer that is accompanied by side effects (Feng *et al.*, 2010; Bradley *et al.*, 2008). Hence, even if it preferentially targets the tumor, one cannot eliminate the possibility of some over-acute reactions in normal tissues when motexafin gadolinium is involved in a treatment procedure.

4.2. Co-toxicity depending on the energy of X-rays

Intriguingly, in this paper, some co-toxicity from the combination of radiation and photoactivatable drugs was observed with 250 kV X-rays, whereas it would be expected that the toxicity would arise from low-energy X-rays that induce a photoelectric effect, and Auger electrons cascade, more probable at the K-edge. To explain this apparent paradox, here are some suggestions. First, like low-energy X-rays, high-energy photons or 200–300 kV X-rays were also shown to trigger cellular membrane permeabilization (Szumiel *et al.*, 1990; Soloviev *et al.*, 2005). Second,

for high-energy photons and 200–300 kV X-rays, it was suggested that photons and electrons resulting from the Compton effect produce low-energy secondary particles that can partially induce a photoelectric effect and damage Auger electron emission (Corde *et al.*, 2003; Biston *et al.*, 2009; Foray, 2011). Finally, our previous report suggested that the co-toxicity after synchrotron radiation tuned to the absorption edge appears to be more significant than that from standard high-energy γ - or X-rays (Biston *et al.*, 2009; Foray, 2011). Our findings in the synchrotron studies suggest the importance of tuning the X-ray energy. For platinated drugs, it appears that the yield of HDCs is greater the closer the X-ray energy is to the Pt K-edge. This result is important because the radiobiological features of the photoactivation of cisplatin tuned to the exact energy at the K-edge (78.4 keV) have not been tested yet. PAT data have only been available at energies of 78.0 and 78.8 keV. The data presented here suggest that the maximal photoactivation effect may be derived by photons whose *exact* energies lie immediately at the K-edge, instead of energies even slightly higher than those at the K-edge. Consequently, with no current data available at 78.4 keV, it seems that the photoactivation of platinated drugs still requires optimization. The conclusion that the maximal effect should be reached with energies immediately at the K-edge has been documented in the literature for other elements, such as calcium, phosphorus and bromide, with which the authors have observed maximal cytotoxicity at the K-edge of the element (Foray, 2010, 2011).

Table 1

Recapitulation of radiobiological properties of the major photoactivatable drugs tested in this study.

Photoactivatable drug	Spontaneous cellular penetrability	DNA-binding capacity of the non-irradiated drug	Radiation-induced cellular penetrability	Toxicity of radiolysis compounds	Mix time post-irradiation for maximal effect
Cisplatin	Yes	Yes	Yes	No?	10 min to 1 h
IUdR	Yes	Yes	Yes	Yes?	10 min
Iomeprol	No	No	Yes	Yes	10 min
Motexafin gadolinium	Yes?	Not known	Yes	Yes	10 min

4.3. Co-toxicity and HDCs

The significance of the observed HDCs needs to be explained. In a model, published in 2008, with 40 quiescent human cell lines that represented one of the largest spectra of human radiosensitivity studied, we proposed that DSB repair could be the result of the interplay between NHEJ and the recombination-like MRE11-dependent pathway. Whenever NHEJ is inhibited, the MRE11 nuclease activity may be exacerbated and lead to the formation of additional DNA single- and double-strand breaks (Joubert *et al.*, 2008). Interestingly, previous reports about iodine (Joubert *et al.*, 2005) and cisplatin (Biston *et al.*, 2004), together with the present data about IUdR, suggest that the combination of irradiation and photoactivatable drugs inhibits NHEJ activity. It was already verified that, like human fibroblasts, the endothelial HMEC cells obey the same mechanistic DSB repair model described above (Joubert *et al.*, 2005). Consequently, the number of DSBs observed in HDCs may be explained by an overactive MRE11 nuclease. Furthermore, the observation that the size of the HDC nucleus appeared to be larger than that of non-HDC cells is in agreement with an excess of DSBs that may cause severe chromatin decondensation (Chavaudra *et al.*, 2004). In addition to these molecular considerations, it must also be considered that the mean free path of PAT-induced Auger electron emission in living matter has a very short range (some nm to μm). Hence, PAT involving platinated drugs (cisplatin and carboplatin) was shown to produce additional DSBs in the immediate vicinity of DNA Pt-adducts. Consequently, a non-random distribution of abnormally small (10–100 kb) DNA fragments are produced along the DNA. This high concentration of small DNA fragments was shown to inhibit NHEJ (Biston *et al.*, 2004, 2009). Hence, both molecular and biochemical processes would be consistent with the production of HDCs specific to PAT, and may explain a significant part of the supra-additive effects of PAT observed with energies around the Pt *K*-edge by comparison with radiation or drug applied separately. HDCs are not apoptotic cells since the shape of nuclei in DAPI-staining did not reveal fragmentation during immunofluorescence experiments and no significant increase of sub-G1 cell subpopulation was observed with flow cytometry. However, one cannot exclude the consideration that long-term HDCs may die in an apoptotic-like process. Further investigations of the destiny of HDCs at periods longer than 24 h post-irradiation are needed to determine the factors involved.

Since chemotherapy drugs do not necessarily show the same cellular penetrability properties, bystander effects should also be considered in the molecular and cellular mechanisms of PAT. Recent investigations of bystander effects have rejuvenated interest in previous demonstrations that irradiation can promote cellular membrane depolarization accompanied by extracellular Ca^{2+} release. In fact, the radiation-induced Ca^{2+} release that generally occurs during the first hour post-irradiation enables the spontaneous entry of molecules into cells (Szumiel *et al.*, 1990). Experiments based on the transfer of irradiated or non-irradiated cell culture media have highlighted the existence of late and indirect formation of DSBs owing to this extracellular calcium release (Maguire *et al.*, 2007). The considerable excess of dose induced by PAT modalities warrants further investigation about potential bystander effects occurring during PAT.

5. Conclusions

The present data provide clues for a general model of synchrotron photoactivation of heavy elements (Table 1). In addition to the excess of 10–100 kb DNA fragments pointed out in previous publications (Corde *et al.*, 2003; Biston *et al.*, 2004, 2009), we provided an awareness of the impact of other biochemical events specific to the combination of X-rays with photoactivatable drugs; that is, the highly damaged cells. Excesses of small DNA fragments and HDCs are likely to contribute to the efficiency of anti-cancer PAT modalities. However, our data show the overall necessity to better estimate the toxicity of PAT in normal tissues since the combination of irradiation and photoactivatable drugs may lead to diffusible toxic effects. Indeed, contrast agents like gadolinium and iomeprol are injected intravenously and may propagate toxicity and produce adverse effects while platinated agents target preferentially tumor cells. Anti-cancer modalities involving synchrotron photoactivation require an important series of experiments to assess all aspects of the impact of radiation on the potential drug candidates for PAT before considering their clinical application in humans.

JG is supported by Region Rhone-Alpes. ZB is supported by a PhD fellowship from Roche-France. AJ was supported by the Institut de Radioprotection et de Sûreté Nucléaire. This work was also supported by the Région Rhône-Alpes, the

Association pour la Recherche sur l'Ataxie-Telangiectasie (APRAT), Association pour la Recherche contre le Cancer (ARC), Electricité de France, l'Institut National du Cancer (INCa) and the ETOILE hadrontherapy Project.

References

- Bencokova, Z., Balosso, J. & Foray, N. (2008). *J. Synchrotron Rad.* **15**, 74–85.
- Biston, M. C., Joubert, A., Adam, J. F., Elleaume, H., Bohic, S., Charvet, A. M., Esteve, F., Foray, N. & Balosso, J. (2004). *Cancer Res.* **64**, 2317–2323.
- Biston, M. C., Joubert, A., Charvet, A. M., Balosso, J. & Foray, N. (2009). *Radiat. Res.* **172**, 348–358.
- Bradley, K. A., Pollack, I. F., Reid, J. M., Adamson, P. C., Ames, M. M., Vezina, G., Blaney, S., Ivy, P., Zhou, T., Krailo, M., Reaman, G. & Mehta, M. P. (2008). *Neuro-Oncology*, **10**, 752–758.
- Chavaudra, N., Bourhis, J. & Foray, N. (2004). *Radiother. Oncol.* **73**, 373–382.
- Corde, S., Balosso, J., Elleaume, H., Renier, M., Joubert, A., Biston, M. C., Adam, J. F., Charvet, A. M., Brochard, T., Le Bas, J. F., Esteve, F. & Foray, N. (2003). *Cancer Res.* **63**, 3221–3227.
- De Stasio, G., Rajesh, D., Ford, J. M., Daniels, M. J., Erhardt, R. J., Frazer, B. H., Tyliczszak, T., Gilles, M. K., Conhaim, R. L., Howard, S. P., Fowler, J. F., Esteve, F. & Mehta, M. P. (2006). *Clin. Cancer Res.* **12**, 206–213.
- Fairchild, R. G. & Bond, V. P. (1984). *Strahlentherapie*, **160**, 758–763.
- Feng, X., Xia, Q., Yuan, L., Yang, X. & Wang, K. (2010). *Neurotoxicology*, **31**, 391–398.
- Foray, N. (2010). *Cancer Radiother.* **14**, 145–154.
- Foray, N. (2011). *J. Neurooncol.* **101**, 161–163.
- Foray, N., Marot, D., Gabriel, A., Randrianarison, V., Carr, A. M., Perricaudet, M., Ashworth, A. & Jeggo, P. (2003). *EMBO J.* **22**, 2860–2871.
- Foray, N., Randrianarison, V., Marot, D., Perricaudet, M., Lenoir, G. & Feunteun, J. (1999). *Oncogene*, **18**, 7334–7342.
- Joubert, A., Biston, M. C., Boudou, C., Ravanat, J. L., Brochard, T., Charvet, A. M., Esteve, F., Balosso, J. & Foray, N. (2005). *Int. J. Radiat. Oncol. Biol. Phys.* **62**, 1486–1496.
- Joubert, A., Gamo, K., Bencokova, Z., Gastaldo, J., Rénier, W., Chavaudra, N., Favaudon, V., Arlett, C. & Foray, N. (2008). *Int. J. Radiat. Biol.* **84**, 1–19.
- Kinsella, T. J., Dobson, P. P., Mitchell, J. B. & Fornace, A. J. J. (1987). *Int. J. Radiat. Oncol. Biol. Phys.* **13**, 733–739.
- Maguire, P., Mothersill, C., McClean, B., Seymour, C. & Lyng, F. M. (2007). *Radiat. Res.* **167**, 485–492.
- Miller, R. W., DeGraff, W., Kinsella, T. J. & Mitchell, J. B. (1987). *Int. J. Radiat. Oncol. Biol. Phys.* **13**, 1193–1197.
- Rothkamm, K. & Lobrich, M. (2003). *Proc. Natl Acad. Sci. USA*, **100**, 5057–5062.
- Soloviev, A. I., Tishkin, S. M., Zelensky, S. N., Ivanova, I. V., Kizub, I. V., Pavlova, A. A. & Moreland, R. S. (2005). *Am. J. Physiol. Regul. Integr. Comput. Physiol.* **289**, R755–R762.
- Szumiel, I., Sochanowicz, B. & Buraczewska, I. (1990). *Int. J. Radiat. Biol.* **58**, 125–131.
- Thomas, C., Charrier, J., Massart, C., Cherel, M., Fertil, B., Barbet, J. & Foray, N. (2008). *Int. J. Radiat. Biol.* **84**, 533–548.
- Turcchi, J. J., Henkels, K. M. & Zhou, Y. (2000). *Nucleic Acids Res.* **28**, 4634–4641.